PHILOSOPHICAL TRANSACTIONS A

royalsocietypublishing.org/journal/rsta

Research

Cite this article: Nisbet EG *et al*. 2021 Isotopic signatures of methane emissions from tropical fires, agriculture and wetlands: the MOYA and ZWAMPS flights. *Phil. Trans. R. Soc. A* **380**: 20210112.
https://doi.org/10.1098/rsta.2021.0112

Received: 29 March 2021
Accepted: 11 August 2021

One contribution of 10 to a discussion meeting issue 'Rising methane: is warming feeding warming? (part 2)'.

Subject Areas:
atmospheric chemistry, environmental chemistry, atmospheric science, biogeochemistry

Keywords:
atmospheric methane, African wetlands, African biomass burning, African air pollution, methane isotopes, aircraft surveys

Authors for correspondence:
Euan G. Nisbet
e-mail: e.nisbet@rhul.ac.uk
Grant Allen
e-mail: grant.allen@manchester.ac.uk

Electronic supplementary material is available online at https://doi.org/10.6084/m9.figshare.c.5680503.

THE ROYAL SOCIETY PUBLISHING

Downloaded from https://royalsocietypublishing.org/ on 27 January 2022

Isotopic signatures of methane emissions from tropical fires, agriculture and wetlands: the MOYA and ZWAMPS flights

MOYA/ZWAMPS Team[1], Euan G. Nisbet[1], Grant Allen[2], Rebecca E. Fisher[1], James L. France[1,16], James D. Lee[3], David Lowry[1], Marcos F. Andrade[4,17], Thomas J. Bannan[2], Patrick Barker[2], Prudence Bateson[2], Stéphane J.-B. Bauguitte[5], Keith N. Bower[2], Tim J. Broderick[6], Francis Chibesakunda[7], Michelle Cain[8], Alice E. Cozens[1], Michael C. Daly[9], Anita L. Ganesan[10], Anna E. Jones[16], Musa Lambakasa[7], Mark F. Lunt[11], Archit Mehra[2,18], Isabel Moreno[4], Dominika Pasternak[3,19], Paul I. Palmer[11,20], Carl J. Percival[15], Joseph R. Pitt[12], Amber J. Riddle[1], Matthew Rigby[13], Jacob T. Shaw[2], Angharad C. Stell[10], Adam R. Vaughan[19], Nicola J. Warwick[14] and Shona E. Wilde[19]

[1]Department of Earth Sciences, Royal Holloway, University of London, Egham TW20 0EX, UK
[2]Centre for Atmospheric Sciences, University of Manchester, Oxford Road, Manchester M13 9PL, UK
[3]National Centre for Atmospheric Sciences, Department of Chemistry, University of York, Heslington, York YO10 5DD, UK
[4]Laboratory for Atmospheric Physics, Institute for Physics Research, Universidad Mayor de San Andrés-UMSA, Campus Universitario, Cota-Cota Calle No 27, La Paz, Bolivia

© 2021 The Authors. Published by the Royal Society under the terms of the Creative Commons Attribution License http://creativecommons.org/licenses/by/4.0/, which permits unrestricted use, provided the original author and source are credited.

Downloaded from https://royalsocietypublishing.org/ on 27 January 2022

[5]Facility for Airborne Atmospheric Measurement, Cranfield University, College Road, Cranfield MK43 0AL, UK
[6]19 Jenkinson Road, Chisipite, Harare, Zimbabwe
[7]Geological Survey of Zambia, Ministry of Mines and Mineral Development, PO Box 50135, Ridgeway, Lusaka, Zambia
[8]Centre for Environment and Agricultural Informatics, Cranfield University, College Road, Cranfield MK43 0AL, UK
[9]Department of Earth Sciences, University of Oxford, South Parks Road, Oxford OX1 3AN, UK
[10]School of Geographical Sciences, University of Bristol, Bristol BS8 1SS, UK
[11]School of GeoSciences, University of Edinburgh, Edinburgh EH9 3FF, UK
[12]School of Marine and Atmospheric Sciences, Stony Brook University, Stony Brook, NY 11794, USA
[13]School of Chemistry, University of Bristol, Bristol BS8 1TS, UK
[14]Department of Chemistry, University of Cambridge, Lensfield Road, Cambridge CB2 1EW, UK
[15]Now at Jet Propulsion Laboratory, California Institute of Technology, Pasadena, CA 91109, USA
[16]British Antarctic Survey, Natural Environment Research Council, Cambridge CB3 0ET, UK
[17]Department Atmospheric and Oceanic Sciences, University of Maryland, College Park, MD 20742, USA
[18]Now at Faculty of Science and Engineering, University of Chester, Chester, UK
[19]Wolfson Atmospheric Chemistry Laboratories, Department of Chemistry, University of York, York YO10 5DD, UK
[20]National Centre for Earth Observation, University of Edinburgh, Edinburgh EH9 3FF, UK

EGN, 0000-0001-8379-857X; GA, 0000-0002-7070-3620; JLF, 0000-0002-8785-1240; PB, 0000-0001-8754-4278; MC, 0000-0003-2062-6556; MCD, 0000-0002-3426-0164; PIP, 0000-0002-1487-0969; JRP, 0000-0002-8660-5136; ACS, 0000-0003-0349-2859

We report methane isotopologue data from aircraft and ground measurements in Africa and South America. Aircraft campaigns sampled strong methane fluxes over tropical papyrus wetlands in the Nile, Congo and Zambezi basins, herbaceous wetlands in Bolivian southern Amazonia, and over fires in African woodland, cropland and savannah grassland. Measured methane $\delta^{13}C_{CH_4}$ isotopic signatures were in the range −55 to −49‰ for emissions from equatorial Nile wetlands and agricultural areas, but widely -60 ± 1‰ from Upper Congo and Zambezi wetlands. Very similar $\delta^{13}C_{CH_4}$ signatures were measured over the Amazonian wetlands of NE Bolivia (around −59‰) and the overall $\delta^{13}C_{CH_4}$ signature from outer tropical wetlands in the southern Upper Congo and Upper Amazon drainage plotted together was -59 ± 2‰. These results were more negative than expected. For African cattle, $\delta^{13}C_{CH_4}$ values were around −60 to −50‰. Isotopic ratios in methane emitted by tropical fires depended on the C3 : C4 ratio of the biomass fuel. In smoke from tropical C3 dry forest fires in Senegal, $\delta^{13}C_{CH_4}$ values were around −28‰. By contrast, African C4 tropical grass fire $\delta^{13}C_{CH_4}$ values were −16 to −12‰. Methane from urban landfills in Zambia and Zimbabwe, which have frequent waste fires, had $\delta^{13}C_{CH_4}$ around −37 to −36‰. These new isotopic values help improve isotopic constraints on global methane budget models because atmospheric $\delta^{13}C_{CH_4}$ values predicted by global atmospheric models are highly sensitive to the $\delta^{13}C_{CH_4}$ isotopic signatures applied to tropical wetland emissions. Field and aircraft campaigns also observed widespread regional smoke pollution over Africa, in both the wet and dry seasons, and large urban pollution plumes. The work highlights the need to understand tropical greenhouse gas emissions in order to meet the goals of the UNFCCC Paris Agreement, and to help reduce air pollution over wide regions of Africa.

This article is part of a discussion meeting issue 'Rising methane: is warming feeding warming? (part 2)'.

Downloaded from https://royalsocietypublishing.org/ on 27 January 2022

1. Introduction

The objectives were to measure methane in air over major tropical sources, especially African wetlands, regional agriculture and biomass burning, to determine at regional scale the characteristic isotopic signatures of these methane sources, and thereby to help constrain regional methane source fluxes and their roles in global methane budget.

There is strong evidence to suggest increasing tropical biological sources such as ruminants and wetlands are major drivers of methane's recent growth [1–4]. Growth in tropical methane emissions is consistent with a widening of regions experiencing tropical climate [5], land-use intensification and rapid population rise coupled with explosive urban growth.

The causes of the recent rapid growth in the atmospheric methane burden, and concurrent isotopic shift to values more depleted in 13C remain poorly understood [1,2,16]. Much of the current rise in the global methane burden is led from sources in the tropics [2–4].

Major tropical methane sources such as wetlands and cattle emit methane isotopically depleted in 13C compared to the bulk global source [2,3,34]. Methane emissions from tropical fires are also significant. But, though isotopic source signatures are key inputs needed if isotopic modelling is to help impose better constraints on global methane budgets, there have been very few studies of the isotopic signatures of methane sources emitting into tropical air masses, especially over central Africa.

Global methane budgets (e.g. [8]) are primarily 'bottom-up' aggregates of on-ground emissions estimates. They are unconstrained or only weakly constrained by isotopic balancing, a difficult task because isotopic data are very sparse from the tropics, especially the African tropics. The 'top-down' measurements reported here, made directly from the air or *in situ*, will allow better constraints to be placed on regional scale isotopic source signatures. In particular, methane emissions from tropical wetlands contribute 60–80% of global natural wetland CH_4 emissions [9] but the carbon isotopic signatures ($\delta^{13}C_{CH_4}$) of methane from African wetlands are very poorly known. Better understanding of African wetland and biomass burning $\delta^{13}C_{CH_4}$ signatures will provide critical new data to constrain global isotopic inversions for methane.

Overall, Lunt *et al*. [10] estimated Africa's annual methane emissions between 2010 and 2016 to be around 76–80 Tg yr^{-1}. This compares with total global emissions estimated at around 600 Tg (top down; [8]). Thus, to balance the global methane budget isotopically, understanding African and Amazonian emissions is critically important.

Hitherto most evidence for atmospheric emissions over tropical Africa has been from satellite remote sensing, or from model or desk studies. *In situ* direct measurement of the atmospheric boundary layer is rare in sub-Saharan Africa outside South Africa and Senegal [11]. Remote marine *in situ* observations, satellite remote sensing and measurement-linked modelling on a regional scale all imply very strong methane emissions from tropical regions in Africa and South America [3,10,12–16], but there have been very few direct measurements by well-instrumented aircraft and ground campaigns.

(a) Isotopic signatures

Isotopic signatures are a critical input for using co-constrained isotopic mass balance modelling to understand the global methane budget [17,6]. For example, Schwietzke *et al*. [18] used isotopes to show that emissions from the fossil fuel industry (gas, oil and coal) were 20–60% greater than estimated in inventories.

Using isotopes to constrain global methane budgets and to understand the processes driving the current strong rise in the methane burden depends on having good information about $\delta^{13}C_{CH_4}$ signatures of sources, especially tropical sources. But previously very few measurements have been made in the tropics [19], where much better measurement of $\delta^{13}C_{CH_4}$ signatures is needed to assess wide-area wetland and fire inputs of methane into the ambient tropical air.

Thus the determination of regional $\delta^{13}C_{CH_4}$ isotopic signatures of specific tropical methane sources is a key objective. Although a few $\delta^{13}C_{CH_4}$ source signatures have been measured locally on the ground [20], regional-scale aircraft-based determinations of $\delta^{13}C_{CH_4}$ signatures are lacking.

Downloaded from https://royalsocietypublishing.org/ on 27 January 2022

In particular, low-altitude research aircraft flights such as those reported here permit integrated sampling of complex aggregations of emissions, difficult to assess by spot-sampling on the ground.

Tropical methane sources are diverse. They include emissions from wetlands, agriculture (especially from cattle, and crop waste burning) and large-area dry season fires (mostly human-lit), as well as emissions from the rapidly growing new urban population centres. An important factor that leads to locally distinctive $\delta^{13}C_{CH_4}$ isotopic signatures is the metabolic make up of the local vegetation. Warm tropical grasslands, farms and wetlands are rich in C4 plants such as maize, sugar and papyrus and many pastoral grasses, with carbon contents that are comparatively rich in ^{13}C. By contrast, trees, bushes and some grasses have C3 metabolisms, which discriminate highly against ^{13}C.

Wetland vegetation in both tropical Africa and South America is typically dominated by C4 grasses, especially C4 papyrus in the equatorial zone, although C3 plants such as reeds are also widespread. Decay of rotting C4 organic debris emits methane with comparatively less negative $\delta^{13}C_{CH_4}$ than methane from C3 vegetation. Although very little is known about emission mechanisms, it is likely that in wetlands rich in tall papyrus and reed stems, methane may be emitted not only through ebullition (which is then subject to isotopically fractionating methanotrophy in the water column) but also through plant and tree stem conduits. Thus on-surface chamber measurements may fail to capture accurately the $\delta^{13}C_{CH_4}$ source signatures of emissions from areas with tall plants (like papyrus) and trees; instead, these signatures may be better captured by integrative aircraft sampling in low flights.

Agricultural methane sources in Africa are large and expected to grow further, driven by rapid growth in human populations and fertilizer use. Methane is produced both by farm ruminants and by crop waste burning. Sub-Saharan African ruminant populations (mainly cattle, but also goats and sheep) are very large [21,38,57]. Eructated $\delta^{13}C_{CH_4}$ values in cattle breath depend on feed and pasture species, which are diverse—tropical cattle diets are typically rich in C4 pasture grasses and crop waste from C4 maize, millet, sorghum or sugar but also including C3 grasses, tree leaves and bushes. Biomass burning of crop waste is often of C4 crop plants like maize or sugar in moist regions, or millet waste in drier agriculture, although other crop waste includes C3 yams, sweet potato and palm waste, etc.

Dry season wildfires are widespread in Africa and South America. Incomplete combustion produces methane with $\delta^{13}C_{CH_4}$ values that depend strongly and characteristically on the type of vegetation fuelling the fires (such as C4 grasses or C3 tree-leaf litter), and that typically has much more positive $\delta^{13}C_{CH_4}$ than wetland emissions. In particular, grassland fires (dominantly C4 plants) tend to produce very ^{13}C-rich methane, while methane in smoke from fires fuelled by C3 trees and leaf litter in facultatively deciduous woodland and forest tends to have rather more negative $\delta^{13}C_{CH_4}$ values.

Africa's dense human populations, with fast growing large cites and major landfills, also emit methane. Fires, urban and rural village emissions cause significant local and regional air pollution in Africa [24], but there have been very few measurements of $\delta^{13}C_{CH_4}$ in methane from these sources. Routine annual grass and crop waste fires, and widespread charcoal burning [25] lead to over 40 000 premature deaths annually from biomass burning aerosols [26] and there is poor air quality over wide areas of Africa [11,27,28]. Enhanced trace gas and particle abundances have been measured over major cities: Accra, Lomé, Abijan and Cotonou [29–31], but there have been few airborne campaigns over heavily populated and intensively farmed rural regions in equatorial Africa.

2. Methodology

As part of the UK Natural Environment Research Council's MOYA (The Global Methane Budget—Methane Observations and Yearly Assessment) and ZWAMPS (Quantifying methane emissions in remote tropical settings—Zambian Wetland Atmospheric Methane Production Study) projects, flight missions and associated on-the-ground field campaigns were carried out

Downloaded from https://royalsocietypublishing.org/ on 27 January 2022

in Africa and South America. Flights in Africa used the NERC Facility for Airborne Atmospheric Measurement (FAAM) BAe-146 aircraft, flights in Bolivia used a Twin Otter aircraft operated by the British Antarctic Survey. The flights in Senegal, Uganda and Bolivia were supported by MOYA, and in Zambia by ZWAMPS. Analytical methods are documented in the electronic supplementary material, accessible online at rs.figshare.com.

(a) Campaign locations: Senegal, Uganda, Zambia, Bolivia

Campaign locations are detailed in the electronic supplementary material, including maps and photographs.

The Senegal flights sampled winter fires in the Casamance region of southern Senegal in February/March (winter) 2017. The Casamance is a region of strongly seasonal rainfall, with a prolonged winter drought. The local vegetation [32] includes tropical woodlands (C3 rosewood), grazing land and seasonal cropland.

Uganda has a strong north-south variation of seasonality, climate, vegetation and agricultural types. The MOYA study had four distinct regional target areas:

(1) C4 Papyrus-dominated (*Cyperus papyrus*) (electronic supplementary material, figure SI 10) equatorial wetlands, including the Lake Wamala region which has both wetlands and widespread farming.
(2) Intensively cultivated agricultural central Uganda around Lake Kyoga. Crops include maize, finger millet, sorghum and sugar (C4), as well as cassava (C3–C4 intermediate), sweet potato (C3) and plantains (C3). There are also many cattle and extensive wetlands.
(3) C4 savannah grassland pastures in dry season northern Uganda.
(4) Regional background air over equatorial Lake Victoria (68 000 km^2 area).

In Uganda, preparatory studies were carried out in 2014 in papyrus swamps on the shores of Lake Victoria between Kampala and Entebbe. The aircraft missions reported below were carried out on 24–29 January 2019. Flights were over several different terrains: (i) over equatorial wetlands, during the equatorial region's brief January dry season; (ii) over near-equatorial farming areas with both intensive crop farming and high cattle populations and (iii) over Northern Uganda in the winter dry season, sampling both woodland and savannah grass fires, by flying through large smoke plumes advected from active fires. Linked surface measurement campaigns on the ground took place both in preparatory work and also coincident with the aircraft flights. These campaigns accessed representative sources, with particular focus on Keeling plot determinations of papyrus wetland source signatures.

In Zambia, from 31 January to 4 February 2019 at the height of a very intense summer wet season [33], the main target was to investigate methane emissions from the large outer tropical wetlands. In particular, methane emissions from the Upper Congo basin [34] have had very little study and thus flights over the 11 000 km^2 Bangweulu wetlands [35, 36] of Northern Zambia were the primary target. These very extensive wetlands, which are a major gathering centre for the Congo drainage, have dense C3 reed and C4 papyrus growth. In addition, flights were also carried out over the reed-rich Lukanga (central Zambia; [61]) and Kafue Flat (southern Zambia;[36]) wetlands in the Zambezi river drainage basin [34]. On the ground, sampling campaigns were carried out during the same week in the Lukanga wetlands and around Lusaka.

In addition, parallel on-ground sampling was carried out in Zimbabwe (fires, cattle, landfill) and for cattle in Kenya.

Bolivian sampling flights were over the Mamore River and Llanos de Moxos of North-East Bolivia [39,40], with simultaneous on-surface sample collection. A parallel paper in this collection [41] examines this region in more detail in the wider context of global tropical isotopic signatures from wetlands and rice fields.

Downloaded from https://royalsocietypublishing.org/ on 27 January 2022

(b) Flight details

In Senegal, four survey flights were carried out: labelled C004–C007 (see electronic supplementary material, information). Transects through smoke plumes emanating from active fires were repeated at altitudes from 1000 ft (300 m) to 6000 ft (1800 m). See electronic supplementary material, figures SI 1 and 2 for flight paths, SI 3 for transect measurements, and [42] for further flight, instrumental and sampling details). Numerous fires were seen, some with large smoke plumes and visible fire fronts (electronic supplementary material, figure SI 4). Background conditions were determined by control flights over the Atlantic.

Flights along the coast of Senegal, Gambia, Guinea-Bissau and Guinea intersected multiple smoke plumes in the prevailing easterly wind, demonstrating that regional pollution was present, with very widespread smoke plumes in the boundary layer and lower free troposphere. Transport times of sampled smoke plumes ranged from a few minutes (in one plume overflown at low altitude over an active fire front (electronic supplementary material, figure SI 4)), to 9–12 h for plumes sampled over the ocean [43]. As there was no recent lightning from thunderstorms, fires were presumably human-lit, whether accidentally or deliberately.

In Uganda, flights using the FAAM aircraft were operated out of Entebbe Airport, Uganda (0° latitude), crossing the equator on take-off and landing. Flights took place during the long winter dry season in northern Uganda and during the brief early year relatively dry interval in the equatorial zone. Electronic supplementary material, figures SI 5–7 show flight paths and measurements, electronic supplementary material, figure SI 8 shows isotopic source attributions from plumes intersected in Kyoga transects, and electronic supplementary material, figure SI 9 shows an *in situ* Keeling plot sampled on the ground from a papyrus-dominated swamp at Kajjansi airstrip south of Kampala (electronic supplementary material, figure SI 10). Barker *et al.* [42] give further flight and sampling details.

In Zambia, FAAM flight surveys (electronic supplementary material, figure SI 11) took place in late January and early February 2019, at the height of the summer wet season [32]. Flight C136 over the Bangweulu wetlands (electronic supplementary material, figure SI 12) took place in a single fortunate dry day with very calm weather and vertical air advection during a very strong wet season with sustained heavy regional cloud cover over northern Zambia. Flights over the Lukanga and Kafue Flat wetlands were in a dry interval in a region of lower seasonal rainfall. Electronic supplementary material, figure SI 13a,b shows on-ground conditions in Lukanga swamp. Unfortunately, an aircraft problem cancelled a planned flight to determine emissions from the Lusaka metropolis.

In Bolivia, a few weeks after the Zambian campaign, flights were carried out in early March 2019, using the British Antarctic Survey's Twin Otter aircraft in the Amazonian Llanos de Moxos wetlands, in N.E. Bolivia, at similar latitude and climate setting to the Zambian campaigns. Further details are given by France *et al*. (2021-this volume; [41])

3. Results

(a) Senegal fires—Casamance dry forest

Keeling plot determination [44] of the methane increments in a smoke plume from Flight C005 gave source $\delta^{13}C_{CH_4}$ about -29.9 ± 0.85‰ (figure 1), though varying with some plumes around -28‰, indicating the dominant fuel was C3 leaf litter, not C4 grasses, a finding consistent with the visual observation of burning forest litter. In smoke, enrichments of up to 0.5 ppm for CH_4 and 300 ppb for CO were measured. Barker *et al*. [42] found these fires had mean emission factors units (in g per kg of dry fuel) of 1.8 ± 0.6 for CH_4, 1630 ± 21.4 for CO_2 and 67 ± 14 for CO, with a mean combustion efficiency of 0.94 ± 0.01, and obtained a $\delta^{13}C_{CH_4}$ value of about -34‰ from all regional sources. Wu *et al*. [43] provide further details about the FAAM flights and sampling for the MOYA project, and report aerosol measurements and chemical transformations in biomass burning plumes sampled in the region.

Downloaded from https://royalsocietypublishing.org/ on 27 January 2022

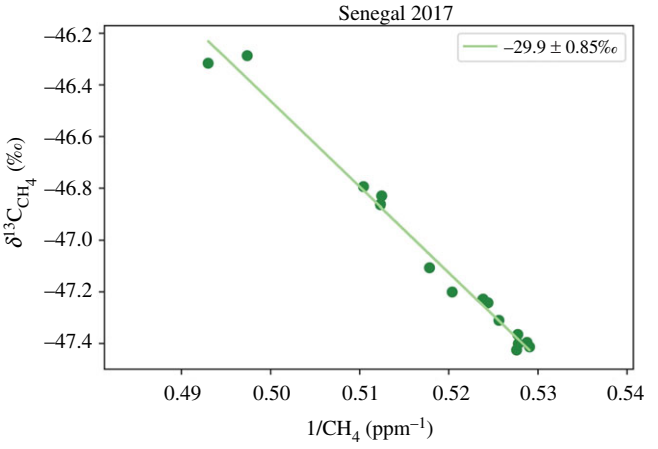


Figure 1. Keeling plot of (1/methane abundance) versus $\delta^{13}C_{CH_4}$ for isotopic measurements of samples in a fire plume on FAAM flight C005 over the Senegal Casamance region. (Online version in colour.)

(b) Uganda—wetlands, savannah and farmlands

There was widespread visual and MODIS-satellite evidence of winter dry season grass fires during the flights over savannah northern Uganda. Significant local methane excesses sampled in air over northern Uganda's grasslands had incremental $\delta^{13}C_{CH_4}$ around −16 to −12‰, indicating the methane sources were indeed C4 grass fires [45]. For these fires, Barker *et al*. [42] found mean emission factors (in $g\,kg^{-1}$) of 3.1 ± 1.6 for CH_4, 1610 ± 52.2 for CO_2 and 78 ± 31 for CO, with a mean combustion efficiency of 0.93 ± 0.03. On one flight a mean N_2O fire emission factor of $0.081 \pm 0.020\,g\,kg^{-1}$ was also measured.

Large methane increments were observed over the wetlands and agricultural districts of central Uganda (electronic supplementary material, figures SI 5,7). For fire plumes over Lake Kyoga, aircraft sampling found methane increments in individual plumes with $\delta^{13}C_{CH_4}$ from −28 to −16‰ (electronic supplementary material, figure SI 8), suggesting the dominant fire fuel was C4 crop waste, such as maize, sorghum and millet, though in some fires perhaps admixed with cassava (C3–C4) or other C3 crop waste, or with emissions from the Kyoga wetlands.

A Miller–Tans plot (following the method of Miller & Tans [46]) of large methane increments (over background) measured in air over Lake Kyoga wetlands and neighbouring agricultural areas (figure 2 and electronic supplementary material, figure SI 7) had $\delta^{13}C_{CH_4}$ of -54.5 ± 1.4‰. Methane in air over the Lake Wamala region of lake wetlands and surrounding farmlands in equatorial Uganda had $\delta^{13}C_{CH_4}$ of -49.3 ± 0.9‰, indicating the methane came from complex mixed sources, likely including the wetlands, crop waste fires and ruminants [38] in this diverse and fertile region. These Miller–Tans plots likely represent regionally representative signals of methane inputs over these complex and varied landscapes.

A prior ground-based sampling campaign in Ugandan wetlands found $\delta^{13}C_{CH_4}$ around -53.0 ± 0.4‰ for methane (electronic supplementary material, figure SI 9) from an equatorial papyrus swamp, though other samples from papyrus wetland near Kajjansi flanking Lake Victoria gave a poorly constrained value of -58.7 ± 4.1‰ [7]. *In situ* sampling was hand-held, and may have failed to access methane emitted from tall papyrus stem tops (3–5 m high) which had bypassed isotopically fractionating methanotrophic uptake in the water column.

Our wetland results compare with −61.2‰ and −62.2‰ values found by Tyler *et al*. [20] from Nyahururu marsh in Kenya. However, like our results over Lake Wamala, Tyler *et al*. [20] also found a range of values in other Kenyan wetlands, from −54‰ to −31‰, although with very high CO_2 measurements in many samples, suggesting complex perturbation.

Downloaded from https://royalsocietypublishing.org/ on 27 January 2022

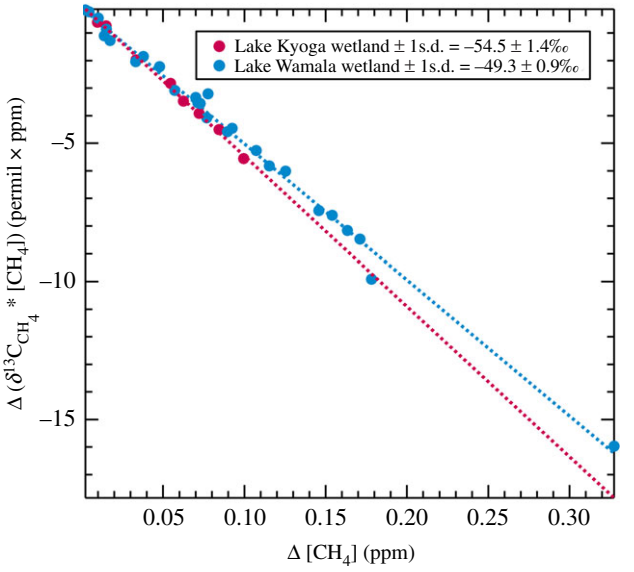


Figure 2. Miller–Tans plots of samples collected in regional air during flights over Lake Kyoga ($\delta^{13}C_{CH_4}$ −54.5 ± 1.4‰) and Lake Wamala ($\delta^{13}C_{CH_4}$ −49.3 ± 0.9‰), Uganda. (Online version in colour.)

Our sampling from East African cattle, to be detailed elsewhere [47], found $\delta^{13}C_{CH_4}$ around −57‰, a range comparable to −57 to −52‰ values we previously found in Zimbabwean cattle [7] and broadly similar to Australian results of −59.7 ± 0.7‰ from grazing cattle, and −62 : 9 ± 1 : 3‰ from feedlot cattle [48]. However, we note our results are significantly more ^{13}C rich than the values around −65‰ found for sub-Saharan Africa by Chang *et al*. [49] (their fig. 4).

(c) Zambia—Bangweulu, Kafue and Lukanga swamps

Strong methane emissions were observed over all the wetlands studied. The Bangweulu transects, flown in still weather conditions with vertical advection of air (see cloud in electronic supplementary material, figure SI 12), measured the highest values over wetlands, not the shallow lake (figure 3*a*,*b*). Isotopic results from 19 air samples collected on the FAAM aircraft over the Bangweulu wetlands found a very well constrained $\delta^{13}C_{CH_4}$ source signature of −59.7 ± 1.3‰ for these Upper Congo wetlands. This may be the first such measurement from the Congo basin.

In the Kafue (Zambezi) basin, figure 4 shows upwind and downwind methane profiles at various altitudes around the Lukanga wetland, providing evidence for significant fluxes of methane from the swamp, perhaps up to 0.3 Tg annually [50]. Over Lukanga, 16 air samples collected on the aircraft gave $\delta^{13}C_{CH_4}$ −62.1 ± 2.3‰.

Parallel on-ground sampling campaigns were also carried out along the margin of the Lukanga swamp, and cattle were widely observed in the wetlands. Unfortunately, the *in situ* isotopic determinations from Lukanga gave complex results, suggesting a diverse range of local sources advecting to the low flying aircraft. Similarly, diverse signatures have also been seen from ground-based work in the Okavango, Botswana [41] and may be related to local burning, variable methanotrophy or locally dominant plant species.

Flights over the third target, the Kafue Flat wetlands, also found substantial emissions with high local methane enhancements. Fire plumes were again observed, marked by elevated CO measurements and indicating a mixed source, although complex local meteorology during sampling of Kafue fluxes makes it difficult unambiguously to separate advected local sources from regional transport of emissions.

Downloaded from https://royalsocietypublishing.org/ on 27 January 2022

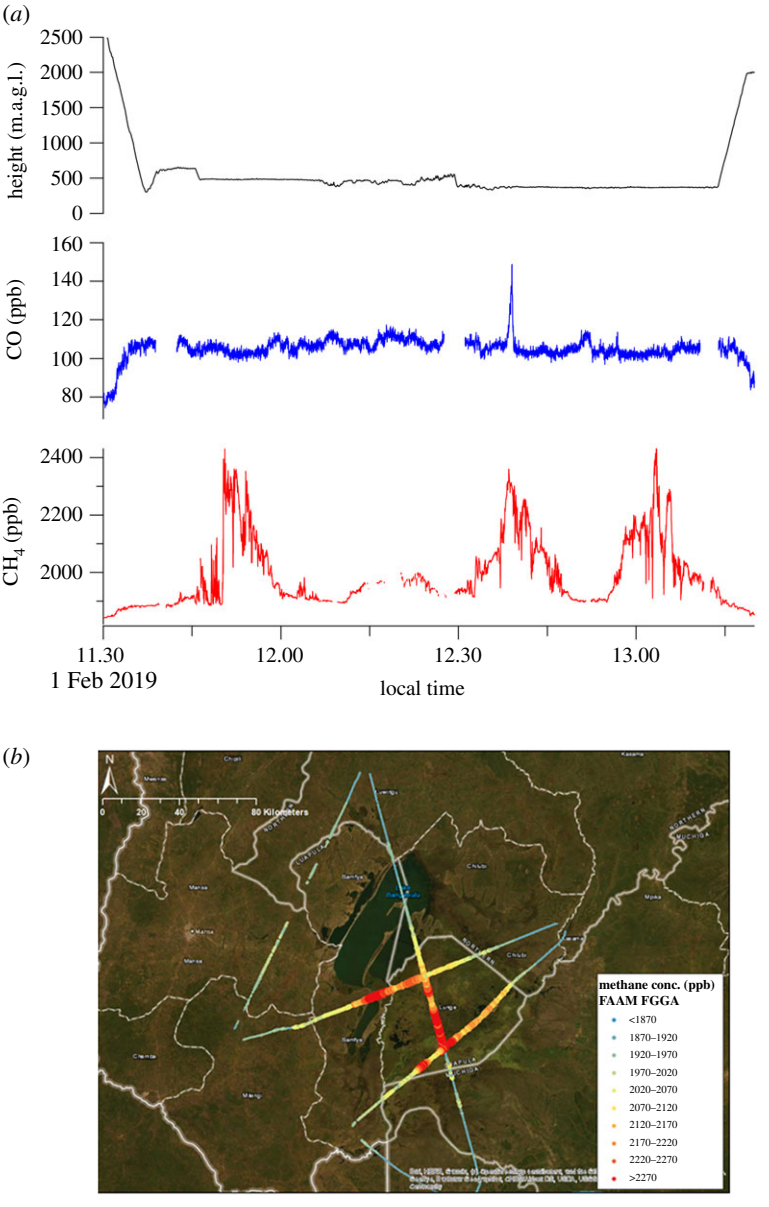


Figure 3. (*a*) ZWAMPS FAAM flight C136, height, CO and methane transects across Bangweulu wetlands. Height is metres above the ground surface. (*b*) ZWAMPS FAAM flight, showing measured methane abundance advected over the Bangweulu wetlands. Transects at various heights above ground level, coloured by *in situ* methane concentration as per legend. Note the highest values are over the wetlands SE of the lake, not over the large shallow lake. (Online version in colour.)

Over the Kafue Flats a Keeling plot of eleven samples collected on board the aircraft gave $\delta^{13}C_{CH_4}$ -60.0 ± 1.2‰.

(d) $\delta^{13}C_{CH_4}$ results from the Mamore River basin, Llanos de Moxos, NE Bolivia

The Bolivian flights measured very large methane enhancements, from which a $\delta^{13}C_{CH_4}$ source signature of -58.7‰ ± 1.9‰ was determined, with similar results from concurrent on-ground *in situ* sampling [41]

Downloaded from https://royalsocietypublishing.org/ on 27 January 2022

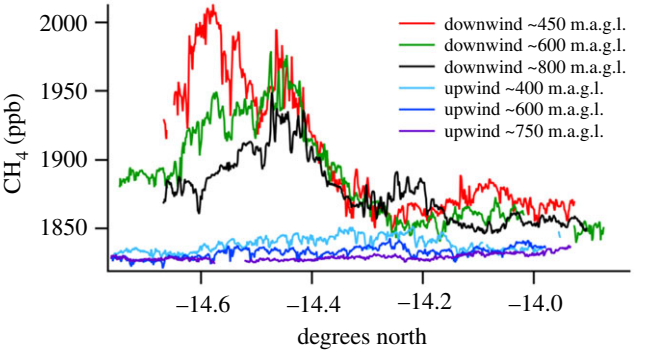


Figure 4. Lukanga swamp. Methane observations during flight transects at various heights above ground level. (Online version in colour.)

4. Interpretation of $\delta^{13}C_{CH_4}$ results

(a) Sahel fires

Prior to the flights over Senegal's southern Casamance region, the expectation had been that the fuel for most fires would be from tropical C4 grasses. That expectation was shown to be wrong from observation during the flights, when it was clear that the fires were primarily in forested areas. This observation was confirmed by the measured $\delta^{13}C_{CH_4}$ −30‰ signature. This value, which is much more negative than likely from C4 grassfires, suggests the primary fuel was leaf litter and fallen or cut wood. The result also suggests that in addition to C4 grasses, C3 tree litter [51] may be a significant fuel for many of the very widespread winter fires across the West African Sahel. This observation is potentially important in the future use of isotopic data to model regional contributions to global methane growth.

(b) Equatorial emissions

The complex isotopic results from aircraft sampling over central Uganda likely reflect the variety of sources over these rich densely populated agricultural regions, with wetlands, large cattle and other animal and human populations, and widespread crop waste and plastic waste fires. The −53‰ $\delta^{13}C_{CH_4}$ values in air samples collected in on-foot fieldwork at water level from equatorial C4 papyrus swamps in Uganda (electronic supplementary material, figures SI 9 and 10) are consistent with the −49 to −55‰ values found in the Miller–Tans plots (figure 2*b*) of air samples collected in flights over the regions around Lake Kyoga and Lake Wamala. However, the relatively ^{13}C-rich measurements over Lake Wamala likely reflect significant inputs from biomass burning.

(c) Southern Hemisphere outer tropics

A Miller–Tans plot of *all* air samples collected over all three Zambian wetlands gave a $\delta^{13}C_{CH_4}$ value of -59.8 ± 1.0‰ ([50] under review). The Zambian and Bolivian wetlands are very comparable. They are at approximately the same latitude in the outer tropics, and sampling was a few weeks apart during the later part of the rainy season in both places, when wetlands were filling. The Miller–Tans isotopic signature reported here from the outer tropical Upper Congo and Zambezi wetlands is very similar to −59‰ values of large methane fluxes measured in the comparable-latitude Bolivian Llanos de Moxos wetlands [41].

Given the similarity between the two regions, a Miller–Tans plot of all data from both areas is justified. Figure 5 shows that when the samples collected over Bolivian Amazonia were included with the Zambian data, the $\delta^{13}C_{CH_4}$ value was -59.3 ± 2.0‰ (figure 5). As a first assumption,

Downloaded from https://royalsocietypublishing.org/ on 27 January 2022

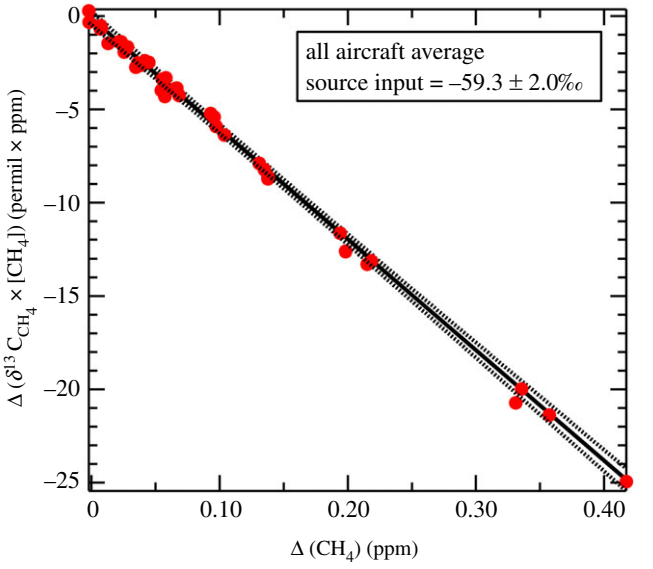


Figure 5. $\delta^{13}C_{CH_4}$ signature of outer tropical wetlands of the Southern Hemisphere. Miller–Tans plot for data from Zambia and Bolivia. The inferred $\delta^{13}C_{CH_4}$ value is -59.3 ± 2.0‰. Plot includes aircraft-collected samples from the Upper Congo (Bangweulu) and Zambezi basin (Lukanga, Kafue) wetlands in Zambia and from the Mamore River and Llanos de Moxos wetlands in Bolivian Amazonia. (Online version in colour.)

this value could be used in global isotopic modelling to represent the outer tropical Southern Hemisphere wetlands.

(d) Mixed sources: how representative are the results?

Our data on East African and Zimbabwean cattle show that the $\delta^{13}C_{CH_4}$ source signatures of African wetlands and ruminant emissions are probably indistinguishable. African wetland regions have significant animal populations, including cattle in the Lukanga swamp (electronic supplementary material, figure SI 13a), and also widespread antelopes (ruminants) and many hippoipotamoi (pseudo-ruminants). Thus the aircraft samples from African wetlands may also include significant eructated methane from ruminants and pseudo-ruminants.

The sampling areas flown over in Zambia and Bolivia were large and thus the overall −59‰ $\delta^{13}C_{CH_4}$ value (figure 5) may be broadly representative of the seasonally moist outer tropical wetlands of both Africa and South America. This −59‰ outer tropical wetland signature is more depleted compared to our previous estimates of the bulk global atmospheric methane source at about −53‰ [13] and the −56.7‰ mean tropical signature used by Ganesan *et al*. [17]. However, these wetland results are comparable in range to our estimates of $\delta^{13}C_{CH_4}$ around −55 to −60‰ emitted from grazing African and Australian cows.

A possible explanation of the contrast between the −49 to −55‰ $\delta^{13}C_{CH_4}$ values found in equatorial Uganda and the -59 ± 2‰ values measured in Zambia and Bolivia is that this may be seasonal, because the Ugandan campaign was carried out in equatorial Uganda's brief relatively dry season in January, and thus likely there was more ^{13}C-rich methane from biomass burning than in wetter periods.

An alternative hypothesis is that the on-ground sampling in Uganda did not properly sample methane advected in papyrus swamps. Methanotrophy in water bodies is selective for $^{12}CH_4$, and it is possible the relatively positive $\delta^{13}C_{CH_4}$ values from the Ugandan on-ground samples, collected approximately 1 m above water level, record methane that is remaining after passing through a zone of methanotrophy during ebullition in the water, but that we failed to sample much less depleted methane channelled directly to the air from the high tops of the 3–5 m high

Downloaded from https://royalsocietypublishing.org/ on 27 January 2022

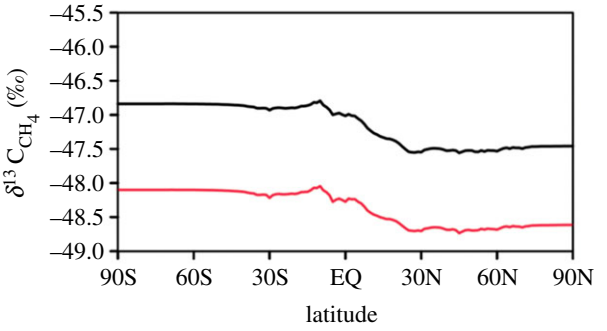


Figure 6. Global impact of changing the $\delta^{13}C_{CH_4}$ source signature of methane emitted from tropical wetlands. Black line (upper line) is a model scenario optimized to NOAA observations with the tropical wetland source having a −55‰ $\delta^{13}C_{CH_4}$ signature. Red line (lower line) shows the impact of changing the tropical wetland source $\delta^{13}C_{CH_4}$ signature from −55‰ to −60‰ on the optimized model scenario, with nothing else varied. (Online version in colour.)

papyrus stalks. By contrast, sampling from low flying aircraft collects bulk emissions and should be more representative of the bulk inputs.

However, a wider hypothesis for the greater ^{13}C depletion measured by the flights in the outer tropics is that these more negative $\delta^{13}C_{CH_4}$ values measured in flights over Zambia and Bolivia are consistent with a broad latitudinal C4 : C3 gradation in plant species, with C4 plants, especially papyrus, dominating in the equatorial wetlands, while in outer tropical Zambia, and in Bolivia, the proportion of C3 reeds and swamp grasses is higher [52].

5. Summary of isotopic signatures

Table 1 summarizes the results from this work and related studies published elsewhere.

6. Modelling

Wetlands are one of the largest global sources of atmospheric methane, estimated to contribute up to approximately 35% of global methane emissions (e.g. [8,53]), with the latitudinal gradient in atmospheric methane mole fractions observed in the NOAA network indicating the bulk of these emissions are situated in tropical rather than high latitude regions. Therefore, atmospheric $\delta^{13}C_{CH_4}$ values predicted by global atmospheric models are sensitive to the $\delta^{13}C_{CH_4}$ isotopic signature applied to tropical wetland emissions.

The evidence presented here shows a latitudinal range in $\delta^{13}C_{CH_4}$ signatures of methane that actually enters the African troposphere, with equatorial emissions being less negative than −55‰, being in bulk derived from wetland vegetation, ruminant fodder and crop waste more rich in C4 species. By contrast, $\delta^{13}C_{CH_4}$ signatures of African outer tropical emissions, from wetlands, pastures and farming somewhat richer in C3 plants, are closer to −60‰, which is similar to the results of the Bolivian measurements, at a latitude very similar to northern Zambia.

This finding has significant impact. Changing the tropical wetland $\delta^{13}C_{CH_4}$ signature from −55‰ (the number currently adopted in many global model studies) to −60‰ in a global atmospheric model [54] resulted in a downward shift in the modelled global surface $\delta^{13}C_{CH_4}$ atmospheric composition of approximately 1.2‰ at steady-state (figure 6). Similarly, adopting −60‰ as the bulk $\delta^{13}C_{CH_4}$ isotopic signature of tropical wetland areas in the analysis of Ganesan *et al*. [17], which employed a different set of global methane fluxes from Warwick *et al*. [54], would shift the modelled global atmospheric $\delta^{13}C_{CH_4}$ value by −0.5‰. Changes of this magnitude are large compared to the measured signals in atmospheric $\delta^{13}C_{CH_4}$ values. Updating the tropical wetland $\delta^{13}C_{CH_4}$ signature to −60‰ in model global budget studies would thus have an important impact on the methane source mixture that best fits the $\delta^{13}C_{CH_4}$ observations.

Downloaded from https://royalsocietypublishing.org/ on 27 January 2022

Table 1. Summary of Isotopic Signatures. Senegal regional value from Barker *et al.* [42], Lake Victoria Swamp value from Brownlow *et al.* [7], Kenyan cattle from Cozens *et al.* [47], Zambia (all) from [50] (under review) and Bolivian wetlands from France *et al.* [41]. All other measurements from this work.

latitude	location	setting	type of vegetation	$\delta^{13}C_{CH_4}$ (‰)
13° N	Senegal—Casamance	biomass burning	C3 woodlands	−29.9 ± 0.9
			leaf litter etc.	
13° N	Casamance	smoke plumes	C3 woodland	−28
13° N	Casamance	regional sources	woodland, arable	−34
3° N	N. Uganda	grassland	C4 fires	−16 to −12
1° N	Central Uganda	farmland fires	C4 and C4 fires	−28 to −16
1° N	Central Uganda Kyoga region	regional	C4 and C3 mixed wetlands and farming	−54.5 ± 1.4
0°	Central Uganda Wamala region	mixed wetlands and farming	C4 and C3	−49.3 ± 0.9
0°	Lake Victoria Wetlands	Kajjansi Swamp	C4 papyrus	−53.0 ± 0.4
0°	Lake Victoria Wetlands	swamp	C4 papyrus	−58.7 ± 4.1
1° S	Kenya	cattle	mixed fodder	around −57
11° S	Zambia—Bangweulu	wetlands	C4 and C3	−59.7 ± 0.7
			papyrus swamps	
14° S	Zambia—Lukanga	wetlands	C3 and C4	−62.1 ± 2.3
16° S	Zambia—Kafue	wetlands	C3 and C4	−60.0 ± 1.2
11–16° S	Zambia (all)	wetlands	C3 and C4	−59.8 ± 1.0
12–15° S	Bolivia	wetland flights	C3 and C4	−58.7 ± 1.9
	Zambia and Bolivia together	flights over wetlands	C3 and C4	−59.3 ± 2.0

While the magnitude of this impact may differ slightly between models depending on the source and sink assumptions, it represents a shift in $\delta^{13}C_{CH_4}$, similar in magnitude to the shift resulting from uncertainties in the tropospheric chlorine sink [55]. Such a modelled shift is much larger than the observed shift in the global burden since 2007 [56]. Thus, the hypothesis that recent vegetation or land-use changes have made equatorial African wetlands emit methane that is isotopically more similar to outer tropical wetlands could in principle explain the post-2007 negative $\delta^{13}C_{CH_4}$ shift in the global burden. This explanation is unlikely, as intuitively a warming climate would drive changes in the opposite direction, but is perhaps worth investigating.

More tropical measurement is needed, to determine the complex effects of seasonality, biomass burning and variations in cattle management and in the C3 : C4 metabolic make up of the surface vegetation [37]. Nevertheless, it is clear that increasing tropical wetland emissions may indeed be an important factor in the explanation of the current negative isotopic shift shown by the global burden [2,3].

7. Discussion

These aircraft and ground measurements have provided direct bulk evidence for the isotopic signature of methane emissions from moist tropical Africa and South America.

Tropical source regions have globally important methane emissions [1,2,3]. In particular, the regions sampled here have very large methane emissions. As part of this work, [50] (submitted)

Downloaded from https://royalsocietypublishing.org/ on 27 January 2022

estimate the Bangweulu wetlands emissions to be around 1.2 Tg of methane annually and the smaller Lukanga swamp in excess of 0.3 Tg yr^{-1}. The methane flux from the Bolivian Llanos de Moxos wetlands may be even greater than the Bangweulu emissions [41]. These very large fluxes are consistent with other estimates. For example, the Nile basin's Sudd wetlands [10,15], which are northern tropical Africa's equivalent of Bangweulu and have similar vegetation, may emit as much as 7 ± 3 Tg annually, although Lunt *et al*. [58] found a smaller flux: 3.5 Tg yr^{-1} in 2018–2019. To put these fluxes into context, they may be compared with total annual UK anthropogenic methane emissions around 2.1 Tg [59].

The magnitude of the Upper Congo Bangweulu fluxes imply the Congo basin, which includes many other similar wetland systems, many at lower and warmer altitudes than Bangweulu, contributes significantly to the isotopic balance of global methane emissions. Lunt *et al*. [10] estimate (their figure 4) that the Congo basin may emit 13 Tg yr^{-1} on average between 2010 and 2016. This number is consistent with a somewhat larger 'guesstimate' by comparison with the Amazon basin, which may emit very roughly 35–40 Tg of methane annually, depending on inter-annual variability, (e.g. see [60]), and if emissions are proportionate to area, the Congo basin, about half its size, would perhaps emit 17–20 Tg annually.

For biomass burning, the values measured and reported here illustrate the importance of identifying the fuel for the fires—whether from C3 plants, relatively richer in ^{12}C, with $\delta^{13}C_{CH_4}$ around −28‰, or from C4 grasses, relatively richer in ^{13}C, with $\delta^{13}C_{CH_4}$ around −16‰ to −12‰. However, what is clear from the flights is the complexity of the sources [61], with intense human activity in all regions where rainfall is adequate to support agriculture. Land surface modelling needs to address this: the sources are multiple and heavily dominated by the impact of human actions: cattle, crop fires, forest fires and C4 : C3 plant ratios all depend on humans.

The state of Africa's atmosphere and its greenhouse gas outputs and their likely responses to climate warming have had little attention: our work shows that this neglect needs to be rectified, particularly given the likely near-future growth in fossil fuel burning and vehicle emissions [62]. In many locations burning is uncontrolled, despite the widespread loss of agricultural nutrients into smoke, and air pollution is widespread in tropical Africa: all problems that demand attention. Although Africa's methane emissions are globally significant, national emissions inventories are as yet poorly constrained for the region. Desk studies are not enough; better measurement is needed. The novel isotopic source signatures for tropical wetlands and fires reported here represent important new co-constraints for use in global methane budget models. Further field measurements are urgently required to improve the representation of the tropics as a key global methane source region.

Data accessibility. Data are archived in CEDA: the UK Centre for Environmental Data Analysis.

Authors' contributions. G.A., J.D.L, T.J.B., Pa.B., Pr.B., J.-B.B., T.J.B., M.C., F.C., A.E.C., M.C.D., R.E.F., J.L.F., M.L., J.D.L., D.L., M.R., A.M., E.G.N., D.P., J.R.P., N.J.W. all took part in flights and/or allied field campaigns on the ground in Africa. France in the air and Andrade and Moreno on the surface carried out Bolivian measurements. G.A. was the lead scientist on all African flights, and France in Bolivia, with Daly, Fisher, France, Lee, Lowry and Nisbet being senior scientists on flights and other campaigns. K.N.B. provided flight planning and flew as mission scientist. M.C. coordinated forecast products with the UK Met Office. A.L.G., M.F.L., P.I.P., M.R., A.C.S. and N.J.W. carried out modelling. N.J.W. prepared figure 6. Shaw, France, Pasternak and Vaughan carried out methane flux quantification from flight campaigns. A.E.J. was PI for Bolivian research. Figure acknowledgements: Banan, Bateson, Fisher, France, Pasternak, Pitt, Vaughan, Warwick. E.G.N. was Project PI for both MOYA and ZWAMPS, conceived of and designed the study, flew in Senegal, undertook preparatory campaigns in Bolivia and Uganda, and drafted and revised the manuscript. Figures 1, 2 and 5 RHUL team; figures 3 and 4 Manchester, York and FAAM teams. Figure 6 N.J.W. Electronic supplementary material photograph credits listed in SI figure captions. SI data plots from on board teams.

Competing interests. The authors declare that they have no competing interests.

Funding. E.G.N. thanks the UK Natural Environment Research Council for grants: NE/S00159X/1 ZWAMPS Quantifying Methane Emissions in remote tropical settings: a new 3D approach. NE/N016238/1 MOYA The Global Methane Budget 2016–2020 and allied consortium grants in partner institutions, and also NE/P019641/1 New methodologies for removal of methane. The team thank the University of Cambridge-Africa ALBORADA research fund for supporting measurements in Kenya.

Downloaded from https://royalsocietypublishing.org/ on 27 January 2022

Acknowledgements. Aircraft flights in Africa were by UK Facility of Airborne Atmospheric Measurements: David Simpson and Maureen Smith, and the exceptional team of pilots and ground crew are all thanked for making these difficult campaigns feasible. Bolivian flights by British Antarctic Survey: thanks to Mark Beasley, Andy van Kitts, Dan Beeden and Rod Arnold, UMSA and the Bolivian government. The Zambian Geological Survey, Ministry of Mines, Zambia is thanked for their very strong support and participation in all stages of the work in Zambia. We thank Solomon Mangeni and the Government of Uganda's National Meteorological Authority of the Ministry of Water and Environment, for their advice, support and help with permits, Steve and Phillipa Forsyth of MAF Uganda gave wise advice and generous hospitality on E.G.N's initial campaign in Uganda, and frequently thereafter, Chacaltaya Observatory team for hospitality in E.G.N's preparatory campaign there; Trish and Lucy Broderick for sampling skills, and Sarah Millington at the UK Met Office for providing forecasting products to aid with flight planning.

References

1. Schaefer H *et al.* 2016 A 21st-century shift from fossil-fuel to biogenic methane emissions indicated by $^{13}CH_4$. *Science* **352**, 80–84. (doi:10.1126/science.aad2705)
2. Nisbet EG *et al.* 2016 Rising atmospheric methane: 2007–2014 growth and isotopic shift. *Glob. Biogeo. Cycles* **30**, 1356–1370. (doi:10.1002/2016GB005406)
3. Nisbet EG *et al.* 2019 Very strong atmospheric methane growth in the 4 years 2014–2017: Implications for the Paris Agreemnt. *Glob. Biogeo. Cycles* **33**, 318–342. (doi:10.1029/2018GB006009)
4. Fujita R, Morimoto S, Maksyutov S, Kim HS, Arshinov M, Brailsford G, Aoki S, Nakazawa T. 2020 Global and regional CH_4 emissions for 1995–2013 derived from atmospheric CH_4, $\delta^{13}C$-CH_4, and δD-CH_4 observations and a chemical transport model. *J. Geophys. Res.: Atmos.* **125**, e2020JD032903. (doi:10.1029/2020JD032903)
5. Staten PW, Lu J, Grise KM, Davis SM, Birner T. 2018 Re-examining tropical expansion. *Nat. Clim. Change* **8**, 768–775. (doi:10.1038/s41558-018-0246-2)
6. Ganesan AL *et al.* 2019 Advancing scientific understanding of the global methane budget in support of the Paris Agreement. *Glob Biogeochem Cycles* **33**, 1475–1512. (doi:10.1029/2018GB006065)
7. Brownlow R, Lowry D, Fisher RE, France JL, Lanoisellé M, White B, Wooster MJ, Zhang T, Nisbet EG. 2017 Isotopic ratios of tropical methane emissions by atmospheric measurement. *Global Biogeochem. Cycles* **31**, 1408–1419. (doi:10.1002/2017GB005689)
8. Saunois M *et al.* 2020 The global methane budget 2000–2017. *Earth Syst. Sci. Data* **12**, 1561–1623. (doi:10.5194/essd-12-1561-2020)
9. Zhu Q *et al.* 2017 Interannual variation in methane emissions from tropical wetlands triggered by repeated El Niño Southern Oscillation. *Glob. Change Biol.* **23**, 4706–4716. (doi:10.1111/gcb.13726)
10. Lunt MF, Palmer PI, Feng L, Taylor CM, Boesch H, Parker RJ. 2019 An increase in methane emissions from tropical Africa between 2010 and 2016 inferred from satellite data. *Atmos. Chem. Phys.* **19**, 14 721–14 740. (doi:10.5194/acp-19-14721-2019)
11. Katoto PD, Byamungu L, Brand AS, Mokaya J, Strijdom H, Goswami N, De Boever P, Nawrot TS, Nemery B. 2019 Ambient air pollution and health in Sub-Saharan Africa: current evidence, perspectives and a call to action. *Environ. Res.* **173**, 174–188. (doi:10.1016/j.envres.2019.03.029)
12. Miller JB, Gatti LV, d'Amelio MT, Crotwell AM, Dlugokencky EJ, Bakwin P, Artaxo P, Tans PP. 2007 Airborne measurements indicate large methane emissions from the eastern Amazon basin. *Geophys. Res. Lett.* **34**.
13. Nisbet EG *et al.* 2021 Atmospheric methane and nitrous oxide: challenges along the path to Net Zero. *Phil. Trans. R. Soc. A* **379**, 20200457. (doi:10.1098/rsta.2020.0457)
14. Miller SM, Michalak AM, Detmers RG, Hasekamp OP, Bruhwiler LM, Schwietzke S. 2019 China's coal mine methane regulations have not curbed growing emissions. *Nat. Commun.* **10**, 303. (doi:10.1038/s41467-018-07891-7)
15. Pandey S, Houweling S, Lorente A, Borsdorff T, Tsivlidou M, Bloom AA, Poulter B, Zhang Z, Aben I. 2021 Using satellite data to identify the methane emission controls of South Sudan's wetlands. *Biogeosciences* **18**, 557–572. (doi:10.5194/bg-18-557-2021)
16. Parker RJ *et al.* 2020 A decade of GOSAT proxy satellite CH_4 observations. *Earth System Science Data* **12**, 3383–3412. (doi:10.5194/essd-12-3383-2020)

Downloaded from https://royalsocietypublishing.org/ on 27 January 2022

17. Ganesan AL, Stell AC, Gedney N, Comyn-Platt E, Hayman G, Rigby M, Poulter B, Hornibrook ERC. 2018 Spatially resolved isotopic source signatures of wetland methane emissions. *Geophys. Res. Lett.* **45**, 3737–3745. (doi:10.1002/2018GL077536)
18. Schwietzke S *et al.* 2016 Upward revision of global fossil fuel methane emissions based on isotope database. *Nature* **538**, 88–91. (doi:10.1038/nature19797)
19. Sherwood OA, Schwietzke S, Arling VA, Etiope G. 2017 Global inventory of gas geochemistry data from fossil fuel, microbial and burning sources, version 2017. *Earth Syst. Sci. Data* **9**, 639–656. (doi:10.5194/essd-9-639-2017)
20. Tyler S *et al.* 1988 Measurements and interpretation of $\delta^{13}C$ of methane from termites, rice paddies and wetlands in Kenya. *Global Biogeochem. Cycles* **2**, 341–355. (doi:10.1029/GB002i004p00341)
21. FAO. 2020 See http://www.fao.org/faostat/en/#data/QA.
22. Uganda Bureau of Statistics. Cattle. See https://www.ubos.org/explore-statistics/2/.
23. Zamstats. 2019 *The 2017/2018 livestock and aquaculture census. Ministry of fisheries and livestock.* Lusaka, Zambia: Central Statistical Office.
24. Marais EA, Wiedinmyer C. 2016 Air quality impact of diffuse and inefficient combustion emissions in Africa (DICE-Africa). *Environ. Sci. Technol.* **50**, 10 739–10 745. (doi:10.1021/acs.est.6b02602)
25. Bockarie AS, Marais EA, MacKenzie AR. 2020 Air pollution and climate forcing of the charcoal industry in Africa. *Environ. Sci. Technol.* **54**, 13 429–13 438. (doi:10.1021/acs.est.0c03754)
26. Bauer SE, Im U, Mezuman K, Gao CY. 2019 Desert dust, industrialization, and agricultural fires: health impacts of outdoor air pollution in Africa. *J. Geophys. Res.: Atmos.* **124**, 4104–4120. (doi:10.1029/2018JD029336)
27. Pfotenhauer D *et al.* 2019 Updated emission factors from diffuse combustion sources in sub-Saharan Africa and their effect on regional emission estimates. *Environ. Sci. Technol.* **53**, 6392–6401. (doi:10.1021/acs.est.8b06155)
28. Lacey FG, Marais EA, Henze DK, Lee CJ, van Donkelaar A, Martin RV, Hannigan MP, Wiedinmyer C. 2017 Improving present day and future estimates of anthropogenic sectoral emissions and the resulting air quality impacts in Africa. *Faraday Discuss.* **200**, 397–412. (doi:10.1039/C7FD00011A)
29. Flamant C *et al.* 2018 The dynamics–aerosol–chemistry–cloud interactions in West Africa field campaign: overview and research highlights. *Bull. Am. Meteorol. Soc.* **99**, 83–104. (doi:10.1175/BAMS-D-16-0256.1)
30. Hopkins JR *et al.* 2009 Direct estimates of emissions from the megacity of Lagos. *Atmos. Chem. Phys.* **9**, 8471–8477. (doi:10.5194/acp-9-8471-2009)
31. Stratmann G, Schlager H, Sauer D, Brocchi V, Catoire V, Baumann R. 2018 Trace gas profiles and anthropogenic plumes from metropolitan areas in West Africa during DACCIWA-Airborne measurements on board the DLR Falcon 20. In *EGU general assembly conference abstracts*, Geophysical Research Abstracts, vol. 20. pp. 19210.
32. Frederiksen P, Lawesson JE. 1992 Vegetation types and patterns in Senegal based on multivariate analysis of field and NOAA-AVHRR satellite data. *J. Veg. Sci.* **3**, 535–544. (doi:10.2307/3235810)
33. Libanda B, Nkolola B, Musonda B. 2015 Rainfall variability over Northern Zambia. *J. Sci. Res. Rep.* **6**, 416–425. (doi:10.9734/JSRR/2015/16189)
34. Daly MC, Green P, Watts AB, Davies O, Chibesakunda F, Walker R. 2020 Tectonic and landscape evolution of Central Africa and implications for a propagating Southwestern Rift in Africa. *Geochem. Geophys. Geosystems* **21**, e2019GC008746. (doi:10.1029/2019gc008746)
35. Bos AR, Ticheler HJ. 1996 A limnological update of the Bangweulu fishery, Zambia. DoF/BF/Report no. 26, Dept. of Fisheries, Zambia.
36. RAMSAR-531. 2020 RAMSAR information sheet 531 (Bangweulu). See https://rsis.ramsar.org/ris/531.
37. RAMSAR-1780. 2020 RAMSAR information sheet 1780 (Lukanga). See https://rsis.ramsar.org/ris/1780,
38. RAMSAR-530. 2020 RAMSAR information sheet 530 (Kafue flats). See https://rsis.ramsar.org/ris/530.
39. Haase R, Beck G. 1989 Structure and composition of savanna vegetation in northern Bolivia: a preliminary report. *Brittonia* **41**, 80–100. (doi:10.2307/2807594)

Downloaded from https://royalsocietypublishing.org/ on 27 January 2022

40. Langstroth Plotkin R. 2012 Biogeography of the Llanos de Moxos: natural and anthropogenic determinants. *Geogr. Helv.* **66**, 183–192. (doi:10.5194/gh-66-183-2011)
41. France J *et al.* 2021 δ^{13}C methane source signatures from tropical wetland and rice field emissions. *Phil. Trans. R. Soc. A* **380**, 20200449. (doi:10.1098/rsta.2020.0449)
42. Barker PA *et al.* 2020 Airborne measurements of fire emission factors for African biomass burning sampled during the MOYA campaign. *Atmos. Chem. Phys* **20**, 15443. (doi:10.5194/acp-20-15443-2020)
43. Wu H *et al.* 2021 Rapid transformation of ambient absorbing aerosols from West African biomass burning. *Atmos. Chem. Phys.* **21**, 9417–9440. (doi:10.5194/acp-2021-49)
44. Pataki DE *et al.* 2003 The application and interpretation of Keeling plots in terrestrial carbon cycle research. *Global Biogeochem. Cycles* **17**, 1022. (doi:10.1029/2001gb001850)
45. Beuning KR, Scott JE. 2002 Effects of charring on the carbon isotopic composition of grass (Poaceae) epidermis. *Palaeogeogr. Palaeoclimatol. Palaeoecol.* **177**, 169–181. (doi:10.1016/S0031-0182(01)00358-3)
46. Miller JB, Tans PP. 2003 Calculating isotopic fractionation from atmospheric measurements at various scales. *Tellus B* **55**, 207–214. (doi:10.3402/tellusb.v55i2.16697)
47. Cozens A *et al.* 2020 Determination of Carbon Isotopic Ratios in Methane from Tropical Ruminants. Unpublished. MSc thesis, Royal Holloway, University of London.
48. Lu X *et al.* 2021 Isotopic signatures of major methane sources in the coal seam gas fields and adjacent agricultural districts, Queensland, Australia. *Atmos. Chem. Phys.* **21**, 10 527–10 555. (doi:10.5194/acp-21-10527-2021)
49. Chang J, Peng S, Ciais P, Saunois M, Dangal SR, Herrero M, Havlík P, Tian H, Bousquet P. 2019 Revisiting enteric methane emissions from domestic ruminants and their δ^{13}C CH_4 source signature. *Nat. Commun.* **10**, 1–14. (doi:10.1038/s41467-018-07882-8)
50. Shaw JT *et al.* Under review. Globally significant methane emissions from African tropical wetlands.
51. Brandt M *et al.* 2020 An unexpectedly large count of trees in the West African Sahara and Sahel. *Nature* **587**, 78. (doi:10.1038/s41586-020-2824-5)
52. Chabwela H, Chomba C, Thole L. 2017 The habitat structure of Lukanga Ramsar site in Central Zambia: an understanding of wetland ecological condition. *Open J. Ecol.* **7**, 406–433. (doi:10.4236/oje.2017.76029)
53. Couwenberg J, Dommain R, Joosten H. 2010 Greenhouse gas fluxes from tropical peatlands in south-east Asia. *Glob. Change Biol.* **16**, 1715–1732. (doi:10.1111/j.1365-2486.2009.02016.x)
54. Warwick *et al.* 2016 Using δ^{13}C-CH_4 and δD-CH_4 to constrain Arctic methane emissions. *Atmos. Chem. Phys.* **16**, 14 891–14 908. (doi:10.5194/acp-16-14891-2016)
55. Strode SA *et al.* 2020 Strong sensitivity of the isotopic composition of methane to the plausible range of tropospheric chlorine. *Atmos. Chem. Phys.* **20**, 8405–8419. (doi:10.5194/acp-20-8405-2020)
56. Lan X, Nisbet EG, Dlugokencky EJ, Michel SE. 2021 What do we know about the global methane budget? Results from four decades of atmospheric CH4 observations and the way forward. *Phil. Trans. R. Soc. A.* **379**, 20200440. (doi:10.1098/rsta.2020.0440)
57. Sage RF, Wedin DA, Li M. 1999 The biogeography of C4 photosynthesis: patterns and controlling factors. *C4 Plant biol.* **10**, 313–376. (doi:10.1016/B978-012614440-6/50011-2)
58. Lunt MF, Palmer PI, Lorente A, Borsdorff T, Landgraf J, Parker RJ, Boesch H. 2021 Rain-fed pulses of methane from East Africa during 2018–2019 contributed to atmospheric growth rate. *Environ. Res. Lett.* **16**, 024021. (doi:10.1088/1748-9326/abd8fa)
59. NAEI. 2021 UK National Atmospheric Emissions Inventory. Methane. See https://naei.beis.gov.uk/overview/pollutants?view=summary-data&pollutant_id=3.
60. Wilson C, Gloor M, Gatti LV, Miller JB, Monks SA, McNorton J, Bloom AA, Basso LS, Chipperfield MP. 2016 Contribution of regional sources to atmospheric methane over the Amazon Basin in 2010 and 2011. *Global Biogeochem. Cycles* **30**, 400–420. (doi:10.1002/2015GB005300)
61. Phiri D, Morgenroth J, Xu C. 2019 Four decades of land cover and forest connectivity study in Zambia—an object-based image analysis approach. *Int. J. Appl. Earth Obs. Geoinf.* **79**, 97–109. (doi:10.1016/j.jag.2019.03.001)
62. Marais EA, Silvern RF, Vodonos A, Dupin E, Bockarie AS, Mickley LJ, Schwartz J. 2019 Air quality and health impact of future fossil fuel use for electricity generation and transport in Africa. *Environ. Sci. Technol.* **53**, 13 524–13 534. (doi:10.1021/acs.est.9b04958)



https://dspace.org/

Isotopic signatures of methane emissions from tropical fires, agriculture and wetlands: the MOYA and ZWAMPS flights

MOYA/ZWAMPS Team; Nisbet, Euan; Allen, Grant; Fisher, Rebecca E.; France, James L. ...

2021-12-06
The Royal Society
https://doi.org/10.1098/rsta.2021.0112
MOYA/ZWAMPS Team, Nisbet EG, Allen G, et al., (2022) Isotopic signatures of methane emissions from tropical fires, agriculture and wetlands: the MOYA and ZWAMPS flights, Philosophical Transactions of the Royal Society A: Mathematical, Physical and Engineering Sciences, Volume 380, Issue 2215, January 2022, Article number 20210112

Downloaded from a DSpace repository. https://dspace.org/